CHINESE OPTICS LETTERS

Vol. 21, No. 9 | September 2023

Water track laser Doppler velocimeter [Invited]

Rong Huang (黄 荣)[1,2], Qi Wang (王 琦)[1,2], Zhiyi Xiang (向志毅)[1,2], Xiaoming Nie (聂晓明)[1,2], Jian Zhou (周 健)[1,2*], and Hui Luo (罗 晖)[1,2]

[1] College of Advanced Interdisciplinary Studies, National University of Defense Technology, Changsha 410073, China

[2] Nanhu Laser Laboratory, National University of Defense Technology, Changsha 410073, China

*Corresponding author: wttzhoujian@163.com

Received April 30, 2023 | Accepted July 27, 2023 | Posted Online September 15, 2023

A water track laser Doppler velocimeter (LDV) is developed with advantages of high update rate, high real-time performance, high concealment, light weight, and small dimensions. The water track LDV measures the advance velocity of the underwater vehicle with respect to the surrounding water. The experimental results show that the water track LDV has an accuracy of 96.4% when the moving velocity of the vehicle with respect to the ground exceeds 0.25 m/s. Thus, the water track LDV is promising in the application of underwater navigation to aid the strapdown inertial navigation system.

Keywords: laser Doppler velocimeter; water track; underwater navigation.
DOI: 10.3788/COL202321.090005

1. Introduction

In underwater navigation applications, the strapdown inertial navigation system (SINS) is the main system to provide attitude, velocity, and position parameters, and the velocity sensor plays a significant role in suppressing the unlimited positioning error growth over time of SINS. A Doppler velocity log (DVL)[1] can provide the velocity of the carrier with respect to the sea bottom (bottom track mode) and the relative velocity of the carrier to water (water track mode). Due to the opacity of the water media for usual radiation types (except for acoustic waves), DVL has become the most widely used speed sensor to aid SINS in underwater autonomous navigation scenarios[2–4]. However, DVL has several disadvantages. First, DVL can hardly meet the requirement of high concealment in military scenarios on account of high transmittance of the water for acoustic waves. Second, real-time requirements cannot be satisfied since the speed of acoustic waves is slow in water (about 1500 m/s). Third, the acoustic wave propagation speed in water is inconstant, influenced by the temperature, salinity, and pressure of the water along the propagation trajectory, resulting in complex correction to the velocity calculated by the DVL. Lastly, a great difference between the velocity update rate of DVL (default 1 or 2 Hz) and the update rate of SINS (usually 100 or 200 Hz) reduces the positioning performance of the SINS/DVL integration system. Therefore, water track velocimeters with lower accuracy but higher concealment, higher real-time performance, and higher update rate are attractive in underwater navigation applications.

Traditional water track velocity sensors basically include an ultrasonic speedometer[5], an optical speedometer[6], an electromagnetic speed log (EML)[7], and a differential pressure-based velocity sensor[8]. The ultrasonic and the optical speedometers are based on the time-of-flight (TOF) method. These sensors monitor the movement time of the tracking particle in water passing through two parallel acoustic beams or optical beams to calculate the speed of the vessel. The accuracy of the TOF velocimeter highly depends on the impurity of the water. The worst situation is that incorrect velocity will be given in muddy or in an aerated water environment. Based on Faraday's law of electromagnetic induction, EML measures the voltage and then translates it into the velocity of the water flow passing through the electromagnetic field. However, the positive and negative electrodes can be easily corroded by water due to direct contact with water. The differential pressure-based velocity sensor measures the differential dynamic pressure at three points on the body of the carrier and then calculates the relative advance speed in water. But the installation requirement of spherical housing limits its applications.

In this Letter, a water track laser Doppler velocimeter (LDV) based on differential laser Doppler velocimetry[9–11] with a forward scattering mode is proposed to measure the advance velocity of the underwater vehicle with respect to surrounding water. The developed water track LDV has high concealment, high real-time performance, light weight, and small dimensions.

LDV has been widely used in many different areas of scientific research and industrial applications to measure various physical parameters since 1964[12], including the velocity of flow[12,13], wind speed[14], vibration[15], and length[16]. In addition, the SINS/LDV integrated navigation system has been applied in land vehicle navigation since 2014[17–21]. However, LDV was not employed in underwater environments to sense the velocity

of the moving vehicle because the laser decays quickly in the water. As a result, it is hard to reach the bottom of the sea to measure the velocity of the vehicle with respect to the seabed. In this Letter, the developed LDV measures the velocity of the vehicle with respect to the water rather than to the sea bottom. To acquire an effective scattering signal from the moving particles in the water, the laser with a wavelength of 532 nm is utilized in the water track LDV, which is in the range of the blue-green window (400 to 550 nm) in ocean water. In addition, the optical scheme is developed with forward-scattering modes, as the scattering coefficient of the laser is the highest in the forward direction according to Mie scattering theory. To the authors' knowledge, this is the first time that LDV has been employed to measure the moving velocity of a vehicle in an underwater environment.

2. Water Track LDV System

The optical structure of a conventional differential LDV with measurements of forward-scattering modes is shown in Fig. 1[9–11]. A Nd:YVO_4 green laser operates in the single longitudinal mode and the TEM00 transverse mode with the wavelength of 532 nm, which is in the range of the blue-green window (400 to 550 nm) in ocean water. The input beam from the laser is split into two parallel beams of equal intensity and equal optical path by an equal optical path beam splitter. After focused by a transmitting lens, two beams intersect and interfere with each other in the measurement volume (MV) to form a set of interference fringes with uniform spacing. The fringe spacing is expressed as $\Delta y = \lambda/2 \sin \alpha$. The parameter λ represents the wavelength of the laser source. $\alpha = \arctan(d/2F)$ is the half intersection angle between two transmitting beams, d is the separation distance of the equal optical path beam splitter, and F is the focal length of the transmitting lens. When scattering particles in the flow travel through the fringes, the forward-scattering light by particles is collected by the receiving lens and detected by the avalanche detector, while two transmitting beams are obstructed by the stop.

The frequency of the forward-scattering signal, called the Doppler frequency, is proportional to the velocity of the flow and inversely proportional to the fringe spacing. Therefore, the relationship between the flow velocity V_{LDV} and the Doppler frequency f_D is given by

$$V_{\mathrm{LDV}} = \frac{\lambda f_D}{2 \sin \alpha}. \tag{1}$$

In order to acquire the Doppler frequency from the signal output by the avalanche detector, several steps should be conducted, as described in Ref. [22]. First, the output signal of the detector passes through a high-pass filter to remove the direct current term. Next, a tracking filter and the fast Fourier transform (FFT) technique are employed to get the spectrum. Frequency spectrum refinement and a correction algorithm are then applied to solve the Doppler frequency precisely. Finally, the velocity of the flow can be calculated based on Eq. (1).

The traditional differential LDV is usually employed to measure the fluid flow velocity in a tube. Thus, the transmitting end and the receiving end are separated at two sides of the tube, which is convenient for the optical alignment between two ends. But in underwater application scenarios, the transmitting end and the receiving end should be bundled with each other when the differential LDV is fixed on the underwater vessel. In order to decrease the length of the total system and increase the waterproofness, four reflectors are employed in the water track LDV system proposed in this Letter, as shown in Fig. 2. All optical and electronic units are placed inside a C-shaped aluminum alloy watertight housing with a transmitting window to emit the transmitting beams and a receiving window to collect the scattered Doppler signal. The photograph of the water track LDV is shown in Fig. 3, of which the dimension is 200 mm × 200 mm × 65 mm and the mass in air is 2.4 kg. The length of the C-shaped measurement groove between the transmitting and receiving windows is 100 mm, and the width is 75 mm.

The LDV body frame (m-frame) is defined by the right-hand rule, as shown in Figs. 1, 2, and 3(b). The origin of m-frame is located at the center of MV. The x-axis is along the bisector of

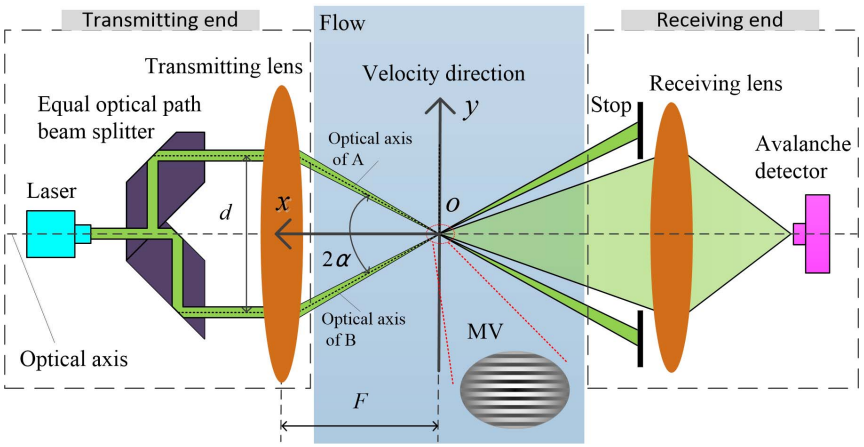

Fig. 1. Basic setup of a conventional differential LDV[9–11].

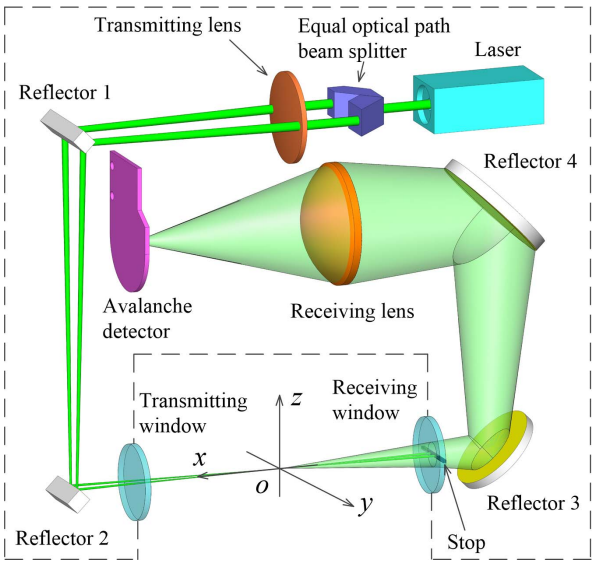

Fig. 2. Optical structure of the water track LDV.

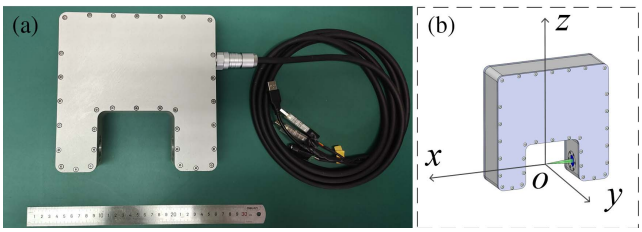

Fig. 3. Photograph of the water track LDV.

the optical axis of A and B. The y axis is in the plane containing the optical axis of A and B and is perpendicular to the x axis. The z axis is perpendicular to the plane containing the optical axis of A and B. As a result, the velocity direction measured by the water track LDV is along the y axis. If this direction is fixed with the axial direction of the moving vehicle, the advance velocity of the vehicle in water can be measured by LDV.

3. Velocity Model of Water Track LDV

The velocity measured by the water track LDV is modeled as follows:

$$\boldsymbol{V}^m_{\mathrm{LDV}} = K_s \widehat{\boldsymbol{V}}^m_{\mathrm{LDV}} + K_b, \tag{2}$$

where $\boldsymbol{V}^m_{\mathrm{LDV}}$ is the true velocity of the moving vessel with respect to the ground and $\widehat{\boldsymbol{V}}^m_{\mathrm{LDV}} = [0,\ V_{\mathrm{LDV}},\ 0]^T$ is the measurement value output by LDV. K_s and K_b denote the scale factor and the velocity bias of LDV output, respectively. $\boldsymbol{V}^m_{\mathrm{LDV}}$ can be replaced by the velocity of $\widehat{\boldsymbol{V}}^m_{\mathrm{GNSS}}$, measured by a highly accurate Global Navigation Satellite System (GNSS). Therefore, Eq. (2) is expressed as

$$\widehat{\boldsymbol{V}}^m_{\mathrm{GNSS}} = K_s \widehat{\boldsymbol{V}}^m_{\mathrm{LDV}} + K_b. \tag{3}$$

From Eq. (3), the calibration model of LDV measurement can be established as

$$V_{\mathrm{GNSS}} = K_s V_{\mathrm{LDV}} + K_b, \tag{4}$$

where $V_{\mathrm{GNSS}} = \|\widehat{\boldsymbol{V}}^m_{\mathrm{GNSS}}\|$ is the velocity measured by GNSS.

The primary polynomial fitting method is applied to estimate the coefficients of K_s and K_b. K_s includes the influence from the shape and the attitude of the watertight housing. In addition, K_s also includes other factors, such as the following coefficient that evaluates how well the natural particles in the water follow the flow motion. The constant component of the current is included in the velocity bias K_b, whereas the random component of the current is ignored in this model.

4. River Test

In order to evaluate the velocity measurement performance of the proposed water track LDV, an experimental test was conducted in the Liuyang River, Changsha, China.

The test facilities are shown in Fig. 4, where a boat is used as the moving vessel. The self-developed water track LDV hangs over the side of the boat and submerges in the water. The measurement direction of LDV is parallel to the axial advance direction of the boat. A high-precision GNSS containing a GNSS receiver, a GNSS antenna, and a 4G antenna is employed to measure the velocity of the vessel in the horizontal direction relative to the Earth as the reference velocity. The measurement data from LDV and GNSS is sent to the Raspberry Pi computer to be processed and saved in the secure digital (SD) card. Additionally, the Raspberry Pi connects to a WiFi transmitter so that real-time velocity of the vessel measured by LDV and GNSS can be monitored via a computer connecting to the WiFi signal. The specifications of related equipment are listed in Table 1.

The test trajectory is shown in Fig. 5, where it starts and ends at the same position: [E113.839330°, N28.325416°]. The duration and the distance of the test are listed in Table 2.

The time history of the velocity is depicted in Fig. 6, where the black line represents the reference velocity sensed by GNSS and the red line is the velocity output by LDV. Besides, the blue line is the simulated velocity (V_y) of MV calculated by the Computational Fluid Dynamics (CFD). The velocity sensed by LDV and the simulated velocity are greater than that by GNSS at most times, indicating that the flow velocity in MV is accelerated by the resistance from the watertight housing of LDV.

The scatterplots of the velocity sensed by LDV and GNSS in the test are depicted in Fig. 7. The velocity outputs by GNSS and LDV are linearly dependent. The Pearson correlation coefficient (PCC) is employed to evaluate the linear dependence between the LDV velocity and GNSS velocity. It is defined as

$$\mathrm{PCC} = \frac{\sum_{i=1}^{n}(X-\bar{X})(Y-\bar{Y})}{\sqrt{\sum_{i=1}^{n}(X-\bar{X})^2}\sqrt{\sum_{i=1}^{n}(Y-\bar{Y})^2}}, \tag{5}$$

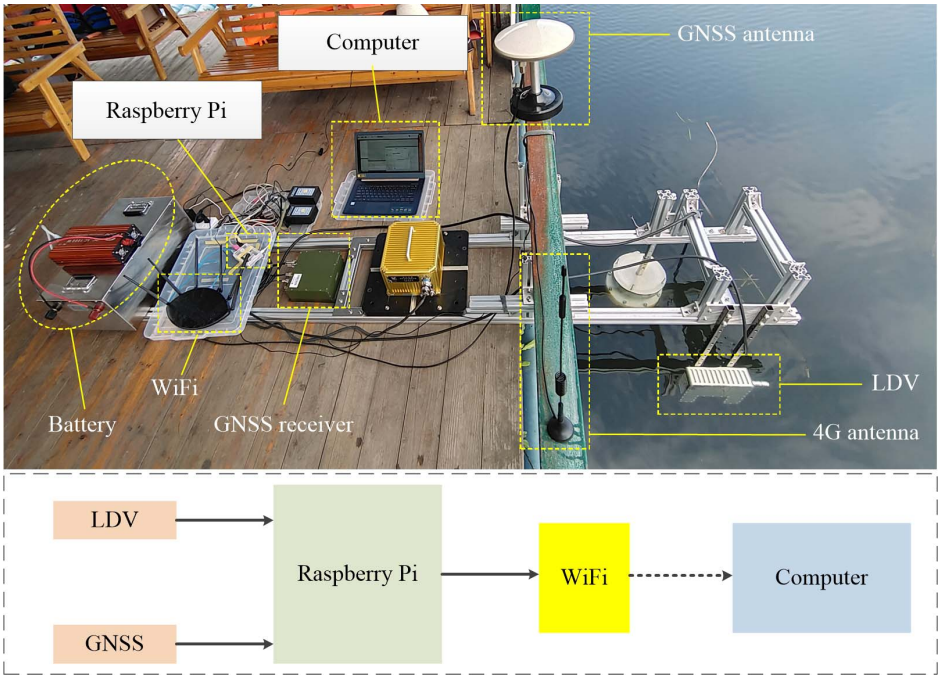

Fig. 4. Photograph of the experiment facilities.

Table 1. Equipment Specifications.

Equipment	Index	Parameter
LDV	Wavelength	532 nm
	Power of the laser	80 mW
	Half intersection angle α	2.748°
	Velocity resolution	3 mm/s
	Data update rate	10 Hz
GNSS	East positioning error	2 cm
	North positioning error	2 cm
	Up positioning error	5 cm
	Velocity error	3 cm/s
	Data update rate	5 Hz

where X and Y are two sets of random variables, and $\bar{X}$ and $\bar{Y}$ are the sample mean of X and Y, respectively. n is the set length of the variable. The PCC of the velocity output by the LDV and GNSS in the river test is 0.9969, indicating that the LDV velocity is strongly linearly correlated with GNSS velocity. Based on the linear model in Section 3, the coefficients of K_s and K_b can be estimated and are listed in Table 2.

To evaluate the estimate accuracy of the linear model, the maximum error (Max), the minimum error (Min), the mean absolute error (MAE), the root mean square error (RMSE),

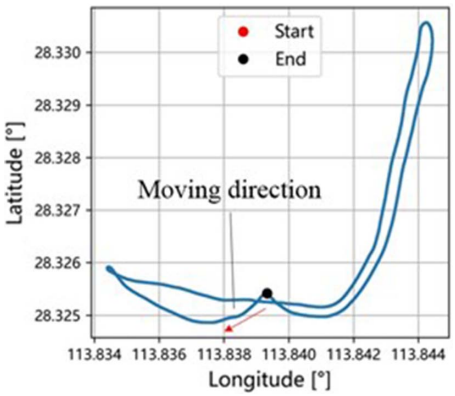

Fig. 5. Trajectory of the river test.

the mean prediction accuracy (MPA), and the relative measurement error (RME) are calculated. They are defined as follows:

$$\mathrm{Max} = \max_n(\tilde{X} - \widehat{X}), \tag{6}$$

$$\mathrm{Mim} = \min_n(\tilde{X} - \widehat{X}), \tag{7}$$

$$\mathrm{MAE} = \frac{1}{n}\sum_{i=1}^{n}|\tilde{X} - \widehat{X}|, \tag{8}$$

$$\mathrm{RMSE} = \sqrt{\frac{1}{n}\sum_{i=1}^{n}|\tilde{X} - \widehat{X}|^2}, \tag{9}$$

$$\mathrm{MPA} = 1 - \frac{1}{n}\sum_{i=1}^{n}\left|\frac{\tilde{X} - \widehat{X}}{\widehat{X}}\right|, \tag{10}$$

Table 2. River Test Results.

Parameters	River Test Result
Duration (s)	3899.6
Distance (m)	3376.1
K_s	0.90153
K_b	0.002334
Max (m/s)	0.218
Min (m/s)	7.211×10^{-7}
MAE (m/s)	0.026
RMSE (m/s)	0.034
MPA (%)	68.8

$$\mathrm{RME}=\left|\frac{\tilde{X}-\widehat{X}}{\widehat{X}}\right|, \tag{11}$$

where $\tilde{X}$ is the estimation of the random variable and $\widehat{X}$ is the true value of the random variable.

The values of evaluating the index for the river test are listed in Table 2. The values of the Max, Min, MAE, and RMSE in the river test are small. However, the MPA is not high. To further evaluate the accuracy of the estimation model, the relationship between the RME and the velocity output by GNSS is depicted in Fig. 8. In the river test, the MPA is −40.2% when the GNSS velocity is within 0.25 m/s. But when the GNSS velocity is greater than 0.25 m/s, the MPA is 96.4%. Figure 8 illustrates that the linear estimation model for the water track LDV is accurate in the high-velocity range. But in the low-velocity range, the estimation ability of the water track LDV is poor.

5. Conclusions

We proposed a water track LDV based on differential laser Doppler velocimetry. The experimental results in the Liuyang River show that the watertight housing of LDV leads to an acceleration in the measurement volume so that the relative velocity measured by the LDV exceeds the velocity over ground. The linear estimation model for the water track LDV has an accuracy of 96.4% when the moving velocity of the vehicle with respect to the ground exceeds 0.25 m/s. To sum up, the water track LDV is practical in that it can estimate the velocity of the

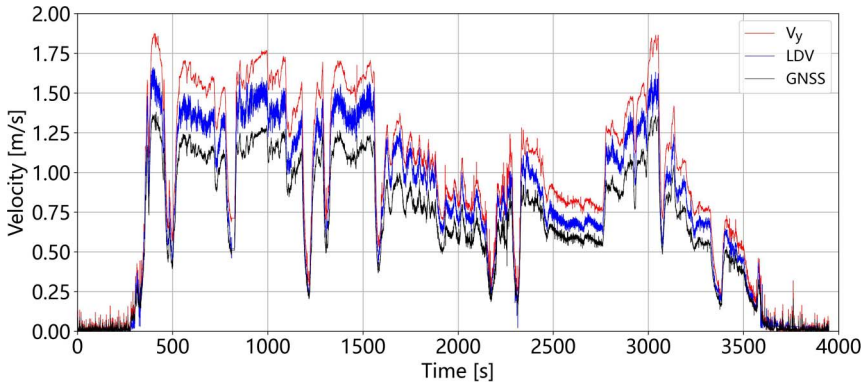

Fig. 6. Velocities output by the LDV and GNSS in the river test and the simulated velocity (V_y) by CFD.

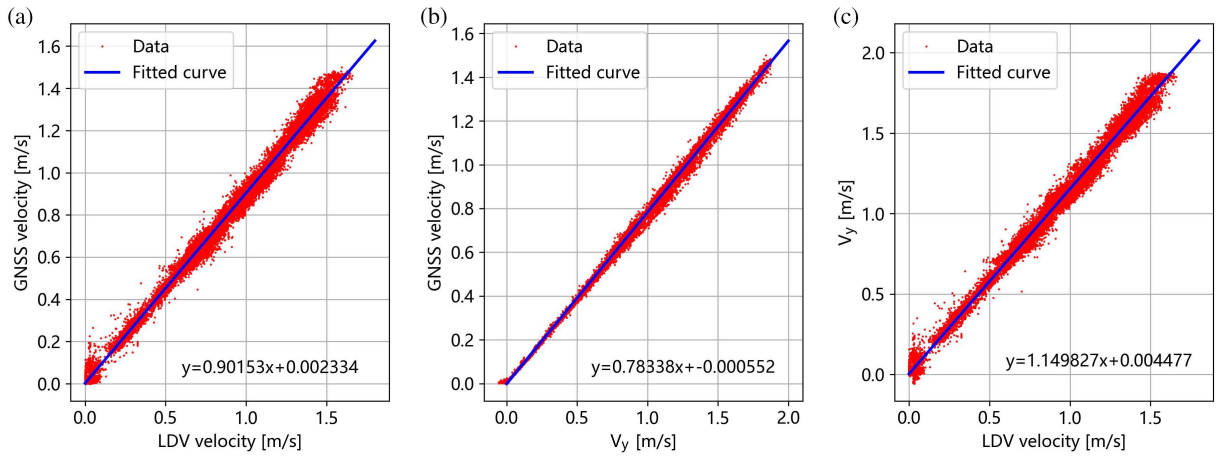

Fig. 7. Velocity scatterplots.

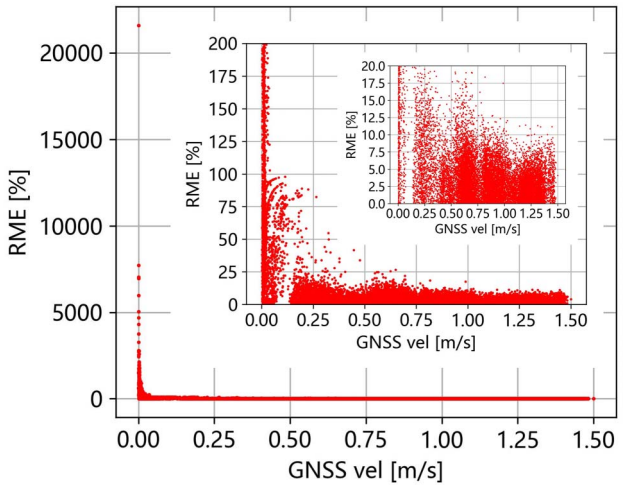

Fig. 8. The relationship between RME and the velocity output by GNSS in the river test.

underwater vehicle when the velocity of the vehicle is larger than 0.25 m/s. And the water track LDV is promising in the application of underwater navigation to aid SINS.

In addition, there is more research that should be conducted in the future, including:

1) The SINS/LDV integrated navigation system should be researched to validate the positioning accuracy of the system in the underwater navigation environment. Considering the drawbacks of DVL in underwater navigation, LDV is a promising sensor to aid SINS in the underwater autonomous navigation applications.
2) Velocity comparison experiments between the underwater LDV and DVL should be carried out to evaluate the velocity measurement accuracy with respect to the water.
3) The shape of the watertight housing of LDV needs to be optimized in order to reduce the influence on the fluid flow.
4) The differential LDV with backward-scattering mode needs to be studied. This type of LDV can be installed inside the carrier with the optical window attached to the housing of the carrier. As a result, there is no influence on the fluid flow from LDV. The difficulty is that the backward-scattering coefficient of laser is small in the water.

Acknowledgement

This work was supported by the Major Basic Autonomous Research Project of College of Advanced Interdisciplinary Studies, National University of Defense Technology, China (No. ZDJC19-12) and the Natural Science Foundation of Hunan Province, China (No. 2021JJ30782).

References

1. P. Liu, B. Wang, Z. Deng, and M. Fu, "A correction method for DVL measurement errors by attitude dynamics," IEEE Sens. J. **17**, 4628 (2017).
2. D. Li, J. Xu, B. Zhu, and H. He, "A calibration method of DVL in integrated navigation system based on particle swarm optimization," Measurement **187**, 110325 (2022).
3. D. Wang, X. Xu, Y. Yao, T. Zhang, and Y. Zhu, "A novel SINS/DVL tightly integrated navigation method for complex environment," IEEE Trans. Instrum. Meas. **69**, 5183 (2020).
4. D. Wang, X. Xu, Y. Yang, and T. Zhang, "A quasi-Newton quaternions calibration method for DVL error aided GNSS," IEEE Trans. Veh. Technol. **70**, 2465 (2021).
5. https://pdf.directindustry.com/pdf/airmar-technology/ust800-ust850-udst800/58581-947913.html.
6. http://www.msesensors.com/papers/microV_description.pdf.
7. M. Emami and M. R. Taban, "A novel intelligent adaptive Kalman filter for estimating the submarine's velocity: with experimental evaluation," Ocean Eng. **158**, 403 (2018).
8. M. Sabet and H. Nourmohammadi, "Water velocity sensor with the ability to estimate the sideslip angle based on Bernoulli's law for use in autonomous underwater vehicles," Ocean Eng. **263**, 112252 (2022).
9. R. L. Bond, *Contributions of System Parameters in the Doppler Method of Fluid Velocity Determination* (University of Arkansas, 1968).
10. M. J. Rudd, "A new theoretical model for the laser Dopplermeter," J. Phys. E Sci. Instr. **2**, 55 (1969).
11. W. T. Mayo, "Simplified laser Doppler velocimeter optics," J. Phys. E Sci. Instr. **3**, 235 (1970).
12. Y. Yeh and H. Z. Cummins, "Localized fluid flow measurements with an He-Ne laser spectrometer," Appl. Phys. Lett. **4**, 176 (1964).
13. M. A. Gondal, J. Mastromarino, and U. K. A. Klein, "Laser Doppler velocimeter for remote measurement of polluted water and aerosols discharges," Opt. Lasers Eng. **38**, 589 (2002).
14. H. Tobben and M. Karbsek, "Experimental and numerical results of optical preamplification in a laser Doppler anemometer receiving head," IEEE Trans. Instrum. Meas. **49**, 10 (2000).
15. M. Martarelli and D. J. Ewins, "Continuous scanning laser Doppler vibrometry and speckle noise occurrence," Mech. Syst. Signal Proc. **20**, 2277 (2006).
16. Ş. K. Özdemir, T. Takasu, S. Shinohara, H. Yoshida, and M. Sumi, "Simultaneous measurement of velocity and length of moving surfaces by a speckle velocimeter with two self-mixing laser diodes," Appl. Opt. **38**, 1968 (1999).
17. J. Zhou, X. Nie, and J. Lin, "A novel laser Doppler velocimeter and its integrated navigation system with strapdown inertial navigation," Opt. Laser Technol. **64**, 319 (2014).
18. Q. Wang, X. Nie, C. Gao, J. Zhou, G. Wei, and X. Long, "Calibration of a three-dimensional laser Doppler velocimeter in a land integrated navigation system," Appl. Opt. **57**, 8566 (2018).
19. M. Wang, J. Cui, Y. Huang, W. Wu, and X. Du, "Schmidt ST-EKF for autonomous land vehicle SINS/ODO/LDV integrated navigation," IEEE Trans. Instrum. Meas. **70**, 8504909 (2021).
20. Z. Y. Xiang, Q. Wang, R. Huang, C. B. Xi, X. M. Nie, and J. Zhou, "Position observation-based calibration method for an LDV/SINS integrated navigation system," Appl. Opt. **60**, 7869 (2021).
21. Z. Y. Xiang, Q. Wang, R. Huang, C. B. Xi, X. M. Nie, and J. Zhou, "A fast robust in-motion alignment method for laser Doppler velocimeter-aided strapdown inertial navigation system," IEEE Sens. J. **22**, 17254 (2022).
22. J. Zhou and X. Long, "Research on laser Doppler velocimeter for vehicle self-contained inertial navigation system," Opt. Laser Technol. **42**, 477 (2010).